Detection and Tracking of Vortices on Oceanographic Images

Isabelle Herlin, Isaac Cohen, Sonia Bouzidi

Detection and Tracking of Vortices on Oceanographic Images

Isaac COHEN Isabelle HERLIN Sonia Bouzidi
INRIA – Rocquencourt
BP 105, 78153 Le Chesnay CEDEX, FRANCE
{Isaac.Cohen|Isabelle.Herlin}@inria.fr

Abstract

This paper deals with the problem of automatic interpretation of oceanographic images for vortices detection, modelization and tracking. We present a framework allowing the vortices detection. The processing is split into three parts: apparent motion computation from the image sequence, local interpretation of apparent motion and geometric modelization of the vortices. This scheme allows an efficient approach for vortices segmentation on very large image sequences. A set of experimental data shows the use of such framework for processing Advanced Very High Resolution Radiometer (AVHRR) and Coastal Zone Color Scanner (CZCS) image sequences.

Keywords: Oceanographic images, Optical flow, Polynomial phase portrait, Geometric modelling, Nonlinear regularization

1 Introduction

Oceanographics images obtained from environmental satellite platforms present a new challenge in computer science. The huge amount of data collected each day and the needs of characterizing some specific structures on these images for oceanographic monitoring justify our approach for the detection and tracking of vortices on oceanographic images.

This paper deals with the problem of automatic interpretation of oceanographic images for vortices detection, modelization and tracking.

We present a framework allowing the vortices detection. The processing is split into three parts:

- Apparent motion computation from the image sequence.
- Local interpretation of apparent motion.
- Geometric modelization of the interesting regions.

This scheme allows an efficient approach for vortices segmentation. The first step concerns the localization of interesting structures on sequences of satellite images. These images are too large (typically 2048×1024 images) for modeling the vortices structures over the whole image. Instead we use an apparent motion computation on oceanographic temporal sequences and characterize the vortices center through a local polynomial approximation of optical flow.

In the regions that have been identified to show a turbulent motion we apply geometric modelization to obtain simultaneously a segmentation of the structures (i.e. the external boundary of the vortex), and a quantitative values (according to the model) allowing a study of the temporal evolution.

The aim of this paper, as it will be explained all over the sections, is to show that dynamic satellite images need a hierarchical approach with two steps, localization and segmentation, due to the large amount data. The paper will also explain our choices for this particular application.

We emphasize that this paper presents fundamental problems arising from applicative and context dependent research in an oceanographic application. Although basic tools like optical flow, vector field interpretation and geometric modelization are presented, we show how these methods can be reformulated and improved to incorporate knowledge of the particular application, like the type of movement occurring on a temperature front or on a vortex.

The paper is organized as follows: section 2 deals with the computation of apparent movement on oceanographic temporal sequences, according to the optical flow equation. In this section, we will discuss the choice of a variational formulation allowing flow discontinuities. These discontinuities characterize oceanographic patterns: temperature fronts and vortices on sea surface temperature images obtained by the Advanced Very High Resolution Radiometer (AVHRR) sensor. In section 3 we present a local polynomial approximation of the flow field, allowing an interpretation of the apparent movement and its fixed points. These points allow to initialize a geometric model of external boundary of the vortex as described in section 4. Finally section 5 presents some results obtained on AVHRR and Coastal Zone Color Scanner (CZCS) images.

2 Optical Flow Computation

Usually [2, 1], the techniques used for computation of optical flow are based on the constant grey level value hypothesis:

$$I = \text{ constant} \tag{1}$$

where I is the grey level value of a pixel.

By differentiating this equation over time when a pixel is apparently moving on an image over a sequence, we obtain:

$$\frac{dI}{dt} = 0 \tag{2}$$

Equation 2 may be rewritten with partial differentiation:

$$\begin{aligned} & \frac{dI}{dt} = \frac{\partial I}{\partial x}\frac{dx}{dt} + \frac{\partial I}{\partial y}\frac{dy}{dt} + \frac{\partial I}{\partial t} && = 0 \\ \iff & \qquad I_x\ u + I_y\ v + I_t && = 0 \end{aligned} \tag{3}$$

where I_x, I_y and I_t are the partial derivatives of the image irradiance function $I(x, y, t)$ at point (x, y) and (u, v) is the velocity of this pixel inside the image. Equation 3 is evidently not sufficient for computing the image velocity (u, v) at pixel (x, y) since the two components u and v are constrained by only one equation, called "optical flow equation". Therefore, most of the techniques make use of a regularity constraint which restrains the space of admissible solutions of optical flow equation, and allows to compute the velocity field on each image of the studied sequence.

Usually, the regularity constraint is quadratics and therefore enforces the optical flow field to be continuous and smooth. For instance, to guarantee a

unique solution to equation 3, one may use a regularizing term by minimizing the energy function:

$$E(u,v) = \int_\Omega (I_x\ u + U_y\ v + I_t)^2 dx + \alpha \int_\Omega |\nabla u|^2 + |\nabla v|^2 dx\ dy \qquad (4)$$

where ∇ denotes the gradient operator. Here, the regularity constraint is applied by a quadratic regularizer $\int_\Omega |\nabla u|^2 + |\nabla v|^2 dx\ dy$ that constrains the optical flow to be usually continuous.

Unfortunately the interesting structures on oceanographic images like temperature fronts and vortices; correspond to discontinuities in the optical flow. This can also be true for other applications where discontinuities occur on the boundary between two surfaces representing two different objects.

A number of authors [4, 8] have studied different methods to allow discontinuities of the optical flow. But most of these approaches require the precomputation of the discontinuity points and a specific processing at these points. For example, equation 4 is used with $\alpha = 0.$, at edge point and with a smooth increase of α in stationary regions to insure the smoothness of the resulting optical flow field. In our application, it is impossible to compute these discontinuity points: on the contrary these points are to be found by use of optical flow.

Naturally, this quadratic regularization is not the only one choice possible. Its use in most cases is due to its simplicity in computation since searching for a minimum of E given by Eq. 4 leads to a set of linear equations.

We have defined a new method for constraining equation 3 (see [5] for a complete description), which is more appropriate since it does not enforce the optical flow to be smooth but guarantees a unique solution. Figure 1 describes on the left, the type of real flow fields occurring on an oceanographic front and on the right, the type of optical flow that would be computed with a continuity constraint.

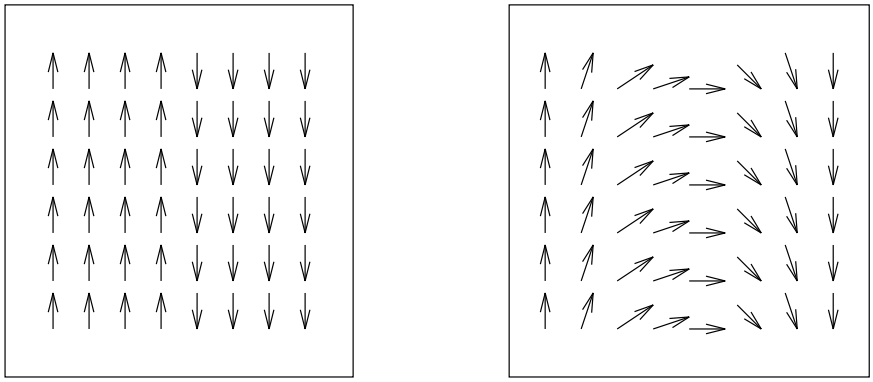

Figure 1: Left: Flow field on a temperature front. Right: Optical flow computed with a continuity constraint.

We are interested in modelling temperature fronts by use of the discontinuity

property. That is not possible if the optical flow is computed with a continuity constraint.

Instead of a quadratic regularizer with L^2 norm ($|u|_2 = \int u^2$) we use a L^1 norm ($|u|_1 = \int |u|$) regularity constraint. L^1 regularizers preserve sharp signals as well as discontinuities. Another advantage is the ability of this model to incorporate additional knowledge such as the characteristics of the noise or the confidence on the stationarity constraint.

We solve the problem of optical flow in the space of functions of bounded variations in $\mathbb{R}^2$; i.e. the space of functions $f = (f_1, f_2)$ such that $\int_\Omega |\nabla f_1| + |\nabla f_2| dx\ dy < +\infty$.

Computation of optical flow (u, v) can now be stated as a minimization of the following energy functional:

$$\int_\Omega \sqrt{\left(\frac{\partial u}{\partial x}\right)^2 + \left(\frac{\partial u}{\partial y}\right)^2} + \sqrt{\left(\frac{\partial v}{\partial x}\right)^2 + \left(\frac{\partial v}{\partial y}\right)^2} dx\ dy + \int_\Omega (I_x\ u + I_y\ v + I_t)^2 dx\ dy \tag{5}$$

This energy minimization problem can be translated into Euler Lagrange form:

$$\begin{cases} -\frac{\partial}{\partial x}\left(\frac{u_x}{\sqrt{u_x^2+u_y^2}}\right) - \frac{\partial}{\partial y}\left(\frac{u_y}{\sqrt{u_x^2+u_y^2}}\right) + (u\ I_x^2 + v\ I_x I_y + I_x I_t) = 0 \\ -\frac{\partial}{\partial x}\left(\frac{v_x}{\sqrt{v_x^2+v_y^2}}\right) - \frac{\partial}{\partial y}\left(\frac{v_y}{\sqrt{v_x^2+v_y^2}}\right) + (u\ I_x I_y + v\ I_y^2 + I_y I_t = 0 \\ + \text{Boundary conditions} \end{cases} \tag{6}$$

Equations in system 6 are non linear and therefore must be processed in a particular way by considering the associated evolution equation, or equivalently, the gradient descend method:

$$\begin{cases} \frac{\partial u}{\partial t} - \frac{\partial}{\partial x}\left(\frac{u_x}{\sqrt{u_x^2+u_y^2}}\right) - \frac{\partial}{\partial y}\left(\frac{u_y}{\sqrt{u_x^2+u_y^2}}\right) + (u\ I_x^2 + v\ I_x I_y + I_x I_t) = 0 \\ \frac{\partial v}{\partial t} - \frac{\partial}{\partial x}\left(\frac{v_x}{\sqrt{v_x^2+v_y^2}}\right) - \frac{\partial}{\partial y}\left(\frac{v_y}{\sqrt{v_x^2+v_y^2}}\right) + (u\ I_x I_y + v\ I_y^2 + I_y I_t = 0 \\ + \text{Boundary conditions} \\ + \text{Initial estimation : } u(0,x,y) = u_0(x,y) \\ \qquad\qquad\qquad\qquad\quad v(0,x,y) = v_0(x,y) \end{cases} \tag{7}$$

In [5], a solution of system 7 is described by a finite element method. This solution is done in two steps, first the temporal discretization of Eq. 7 and then the spatial discretization. This can be done since the temporal variable t and the space variables (x, y) are independent.

3 Motion Interpretation

As explained in the introduction, our aim is to make use of the optical flow, we described in the previous section, to localize interesting regions that have to be further modelized. The extraction of higher level description is necessary to characterize different types of movement.

Different studies have been done on linear phase portrait [9, 6, 7] and their use for characterizing oriented texture field. Zhong et al [10] propose an application of linear phase portrait interpretation of structures in a fluid flow. The main drawback of this method is that it can handle only one critical point. This is inconsistent for our application as we can observe different vortices on the data. Recently Ford and Strickland [11] proposed a nonlinear phase portrait model allowing multiple critical points, but the model seems computationally expensive, and not very stable.

In this paper, we propose a new method for approximating an orientation field and for characterizing stationary points of trajectories obtained from an arbitrary phase portrait.

3.1 Approximation by a polynomial phase portrait model

Suppose that we wish to approximate our optical flow field $f = (u, v)$ by a polynomial phase portrait model

$$g(x,y) = \begin{cases} \dfrac{dx}{dt} &= P(x,y) \\ \dfrac{dy}{dt} &= Q(x,y) \end{cases} \tag{8}$$

where P and $Q \in Q_n(\mathbb{R}^2) = \{p, st\ p(x,y) = \sum_{i,j \leq n} a_{ij} x^i\ y^j\}$.

We fit this model into the original field by minimizing locally an energy function

$$S(g) = \frac{1}{2} \sum_{k,l \in W} |f \times g|^2 \tag{9}$$

where $f \times g$ denotes the cross product of the two vectors f and g and $(k,l) \in W$ is the considered neighborhood.

In the following we show that recovering the coefficients of the two polynomials P and Q by minimizing S amounts to an eigenvalue problem. This approach represents a major advantage since it leads to a linear problem independing of the chosen polynomials P and Q.

Let $X = (x^i y^j)_{i,j=0\ldots n}$ be a basis of $Q_n(\mathbb{R}^2)$, we can write:

$$g(x,y) = \begin{cases} P(x,y) = \sum_{i,j \leq n} a_{i,j} x^i\ y^j = \Omega_a^T X \\ Q(x,y) = \sum_{i,j \leq n} b_{i,j} x^i\ y^j = \Omega_b^T X \end{cases} \tag{10}$$

S can be rewritten as:

$$S(g) = \frac{1}{2}\sum_{W}(\Omega_a^T X f_2 - \Omega_b^T X f_1)^2 \tag{11}$$

Let $B = (Xf_2, -Xf_1)^T$ and $L = (\Omega_a, \Omega_b)$, we have:

$$S(g) = S(L) = \frac{1}{2}\sum_{W}(BL)^2 \tag{12}$$

To obtain the unicity of the solution we add a normalization constraint $L^T L = 1$ and finally the similarity measure between the optical flow field $f = (u, v)$ and the model $g = (\Omega_a X, \Omega_b X)$ is obtained by the minimization under constraint of $S(L)$:

$$S(L) = \frac{1}{2}\sum_{W} L^T\ B^T\ BL + \frac{1}{2}\lambda(L^T\ L - 1) \tag{13}$$

A minimum is characterized by the derivatives equations:

$$\left\{ \begin{array}{lcl} \dfrac{\partial S}{\partial L} & = & B^T\ BL + \lambda\ L = 0 \\ \dfrac{\partial S}{\partial \lambda} & = & \frac{1}{2}(L^T\ L - 1) = 0 \end{array} \right. \tag{14}$$

which lead to the following eigenvector problem:

$$-B^T\ BL = \lambda\ L \tag{15}$$

along with the normalization constraint:

$$L^T\ L = 1 \tag{16}$$

The vector L, representing the coefficients of the model in a polynomial basis, is characterized as the eigenvector associated to the largest eigenvalue of the matrix $-B^T\ B$.

3.2 Interpretation

After approximation of the optical flow field by a polynomial flow field, it becomes possible to characterize some high-level information in the vector field. In the following we report the classification of fixed points for a linear phase model and in the general case of polynomial models. Linear phase models can be used in the neighborhood of fixed points of arbitrary polynomial model as a first order approximation. Indeed, the behavior is the same as for the first order approximation (i.e. linear case) except that when the characteristic roots are pure complex, we have a center or a focus [3]. Nevertheless, the experiments shown in this paper were obtained with a third order polynomial model ($i.e\ Q_3$).

3.3 Linear case

Consider a linear phase model where the polynomials P and Q are in $P_1(\mathbb{R}^2) = \{p \ st \ p(x,y) = a_{00} + a_{10}x + a_{01}y\}$.

The vectors base may be written $X = (1, x, y)$ and the model may be rewritten:

$$\left\{ \begin{array}{rcl} \dfrac{dx}{dt} & = & a_{00} + a_{10}x + a_{01}y = (a_{00}, a_{10}, a_{01})X \\ \dfrac{dy}{dt} & = & b_{00} + b_{10}x + b_{01}y = (b_{00}, b_{10}, b_{01})X \end{array} \right. \tag{17}$$

Once we have recovered at each point the coefficients of the linear model a fixed point x_f can be classified according to the eigenvalues, λ_1 and λ_2, of the matrix $A = \begin{bmatrix} a_{10} & a_{01} \\ b_{10} & b_{01} \end{bmatrix}$, and we obtain the following classification:

- if λ_1 and λ_2 are real:
  - if λ_1 and λ_2 are distinct and of the same sign, then x_f is a node,
  - if $\lambda_1 = \lambda_2 < 0$ or $\lambda_1 = \lambda_2 > 0$, then x_f is a degenerate node,
  - if $\lambda_1\lambda_2 < 0$, then x_f is a saddle point,
  - if $\lambda_1 = \lambda_2 = 0$, then x_f is a singular node,
- if λ_1 and λ_2 are complex:
  - if $Re(\lambda_1) = 0$, then x_f is a center,
  - if $Re(\lambda_1) < 0$, then x_f is a stable focus,
  - if $Re(\lambda_1) > 0$, then x_f is an unstable focus.

In the case of a polynomial model, the previous linear approximation holds in the neighborhood of a fixed point and hence can be used for its classification but it requires the computation of the fixed points *i.e.* the solution of a set of polynomial equations of arbitrary degree. Instead we make use of the index of a flow field.

3.4 Index of a flow field

Let $\mathcal{F} = (P, Q)$ be a vector field defined over a Jordan curve J in the Euclidean plane, with no critical point on J. The index of $\mathcal{F}$ over J is proportional to the angular variation of the vector $\mathcal{F}(M)$ (applied at $M \in J$) as M describes J. For the system (**??**), the index over an oriented Jordan curve J is given by:

$$\text{Index(J)} = \frac{1}{2\pi} \oint_J d\left(\arctan\frac{Q}{P}\right) = \frac{1}{2\pi} \oint_J \frac{PdQ - QdP}{P^2 + Q^2}. \tag{18}$$

A classification of the flow field $\mathcal{F}$ can be obtained by computing the index over a small circle surrounding an isolated critical point. Since it is hard to compute the stationary points of the system (**??**), it leads to solve a system

of polynomials with arbitrary degree. We have chosen to compute locally the index of $\mathcal{F} = (P, Q)$ over the whole flow field. At each point we consider a circle contained in the centered window W and we use the following classification:

- The index of a focus, a center or a node is equal to $+1$,
- The index of a saddle point is -1.

Although this characterization is compendious, it characterizes the most important structures in a fluid flow field. The index measure computed over all the flow allows us also to obtain critical points locations without computing the roots of the system (**??**). Once we located these points we may use the linearization of polynomial model at the neighborhood of fixed points to obtain a complete description of the flow field in these points.

In this approach, we have proposed a two step method based on first computing an optical flow field preserving motion discontinuities and then fit locally a polynomial phase model to the obtained field. We could have used a polynomial model for flow computation [**?**] and its characterization. Using such a model has some limitations. Indeed, flow discontinuities and non uniform tessellation which are two important properties in oceanographic image sequences, cannot be used with a polynomial model.

4 Vortex segmentation and quantification

Optical flow and polynomial phase portrait methods allows to characterize some regions of interest. These regions correspond to node and focus points of the phase portrait model and we will modelize them as vortices in the following.

This modelization is based on the following properties of vortices:

- The region including the vortex is the result of a cold and a warm front meeting: so it is characterized by an important variation of gray level values,
- Edge detection within the image shows that a lot of points on the structure's boundary have a high gradient norm value,
- Variance calculus with application of hysteresis thresholding, allows to localize vortex rolls,
- Geometrically, the external shape of the vortex may be approximated by an arc of a circle.

4.1 Segmentation of the vortex rolls

The rolls of the vortex are small circle-like regions characterized by an important variation of gray level values. We have chosen to extract them by using the variance image, which is defined for each pixel of the data image, by the variance

of a window centered around that point. A window of radius 10 pixels leads to fair results regarding to the size of the studied phenomena.

Regions of interest are then extracted by hysteresis thresholding of that image. Thresholding values are automatically computed as corresponding to the classical 95 percent threshold on the variance histogram.

After this process, we still have to eliminate remaining false regions. We then use the fact that the regions we are searching for, have a small extension and have approximately the shape of a circle -or an ellipse with eccentricity close to -1-. This is done by computing principal directions of the region, and its extensions along those directions. A simple thresholding on the ratio of these extensions is enough to retain only good regions.

4.2 Segmentation Model

We modelize vortices by computing their center regions and by an arc of a circle delimiting their extension. We there use a half of a circle. We then have to determinate, firstly, the center and the orientation of this arc. This depends on the type of vortex and we distinguish two main cases :

- Symmetric case : the vortex is made of two rotating regions evolving in the same way. The extreme points of the arc will be on the axis between centers of gravity of the two regions, and the center will be the center of symmetry of the regions.
- Other cases : only one vortex has evolved enough. We then center the arc over the center of these regions.

The arc must be such that gradient norm is maximal along it. We express that with the help of the following energy functional :

$$E(r) = \frac{1}{2r} \sum \|\nabla I(x(r), y(r))\|^2 \tag{19}$$

where r represents the radius of the circle's arc of our model.

5 Application on oceanographic images

Image processing tools have been applied quite successfully these past few years in the domain of land cartography. The shapes to be extracted are numerous and complex (roads, rivers, airports,..). On the other hand, oceanographic "shapes" have received very few attention up to now. Structures such as fronts and vortices can often be found on sea surface temperatures images (AVHRR). These structures may vary a lot with time, and therefore a specific process is required to detect them. Several problems arise in vortices detection and tracking :

- AVHRR images represent a huge amount of data to process daily. We then need to localize area of interest within a wide image, in order to work on

a smaller one. This suppose that a vortex is never missed, and also that we minimize the number of false hits;

- a mathematical framework for segmenting the structure within the smaller image is required ;
- at last, we need a modelization of structure's shape that allows wide deformations.

This paper has focused on the first and the third points above. We will now present some results obtained on temperature and CZCS images .

We have started our process by a optical flow computation over an AVHRR image sequence. Figure 2 shows an overlay of the obtained displacement field on a frame. Some particular flow patterns can be seen over the whole image. We can distinguish node points, vortex points and saddle points. The purpose of the motion interpretation explained in section 3 is to localize automatically those regions. We have used a cubic polynomial phase portrait to classify the different flow patterns. Figure 3 shows the obtained regions of interest, where grey regions represent nodes and white regions, vortices.

The geometrical modelization is then applied on a small window centered on the region classified as vortices points. The maximization of the energy function described in equation 19 yields on a CZCS image (figure 4), an efficient representation of the vortex. An overlay of the model on the image data is shown in figure 5.

Finally, we have applied our geometric model on CZCS image sequence to characterize the evolution of the spatio-temporal deformable structure. This variation involves position, extension and geometry (and even topology, if two vortices merge for instance) as can be seen in figure 6 showing three successive frames of the image sequence. Those structures have a temporal evolution which depends on their location, size and the period of the year. We expect to use the obtained geometric model to characterize their evolution.

6 Conclusion

This paper has presented a global methodology to localize, segment and track vortices on oceanographic images. We make use of some information on the physical processes occurring on the images. In the future we plan to:

- reconsider the validity of optical flow equation for different applications : would it be possible to make use of a different assumption on the variation of the gray level value?
- compare image processing and geophysical modelling for vortices detection and tracking in order to study if image processing of dynamic satellite image may be an alternative way of processing these data for a daily analysis.

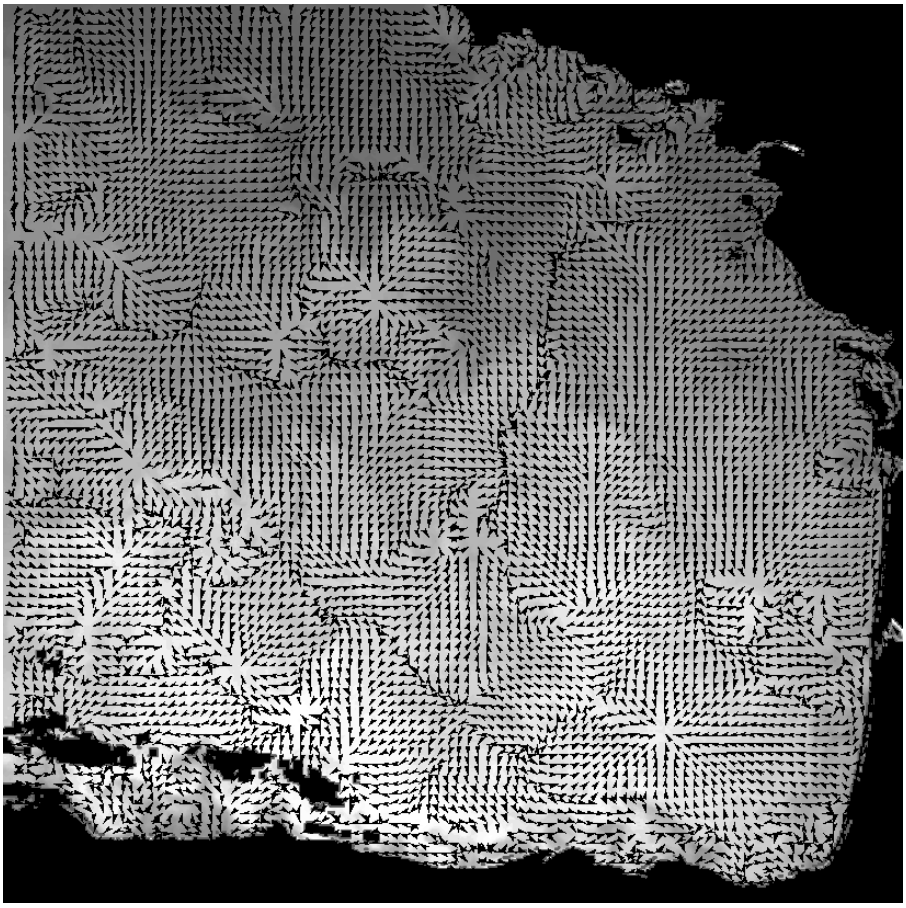

Figure 2: An overlay of the optical flow field and the corresponding AVHRR image.

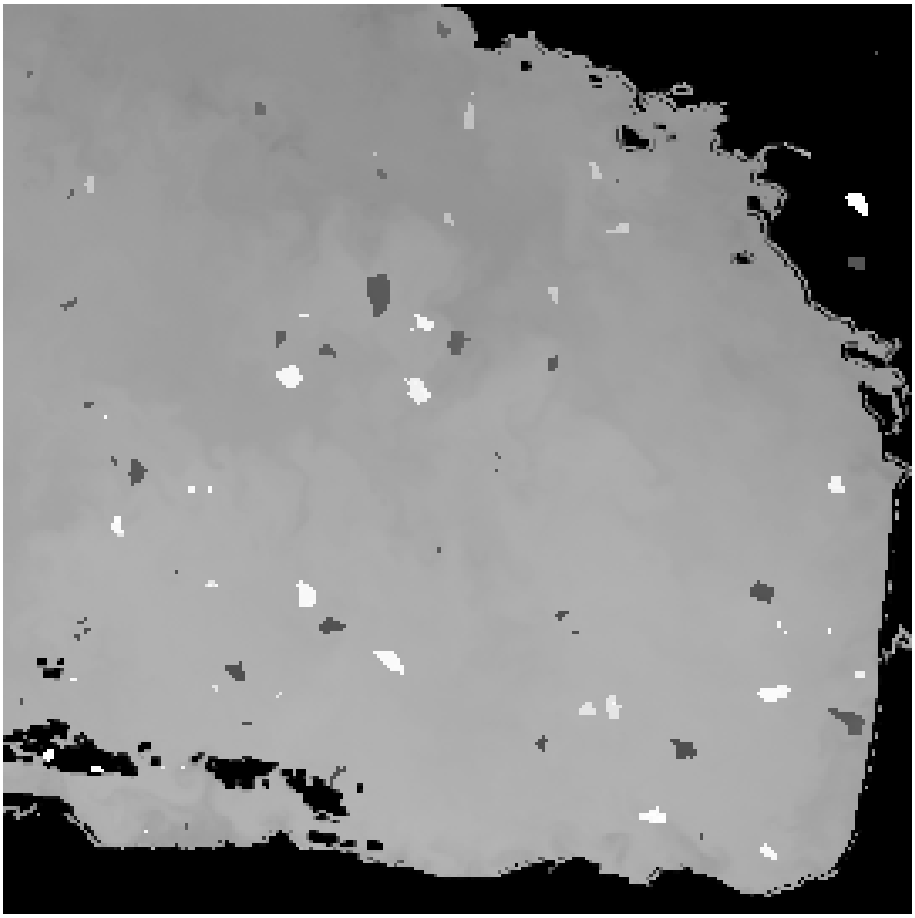

Figure 3: Interpretation of optical flow by a cubic polynomial phase portrait. Gray regions represent nodes while white regions represent vortices.

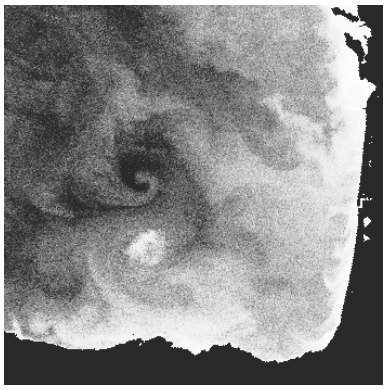

Figure 4: A CZCS image of the western french coast (given by the OCEAN project).

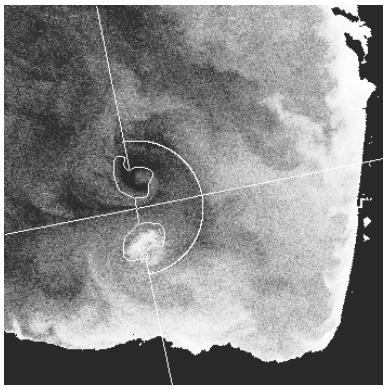

Figure 5: Vortex model applied to a CZCS image after localizing vortex rolls and fitting the arc representing vortex boundaries by maximizing Eq. 19.

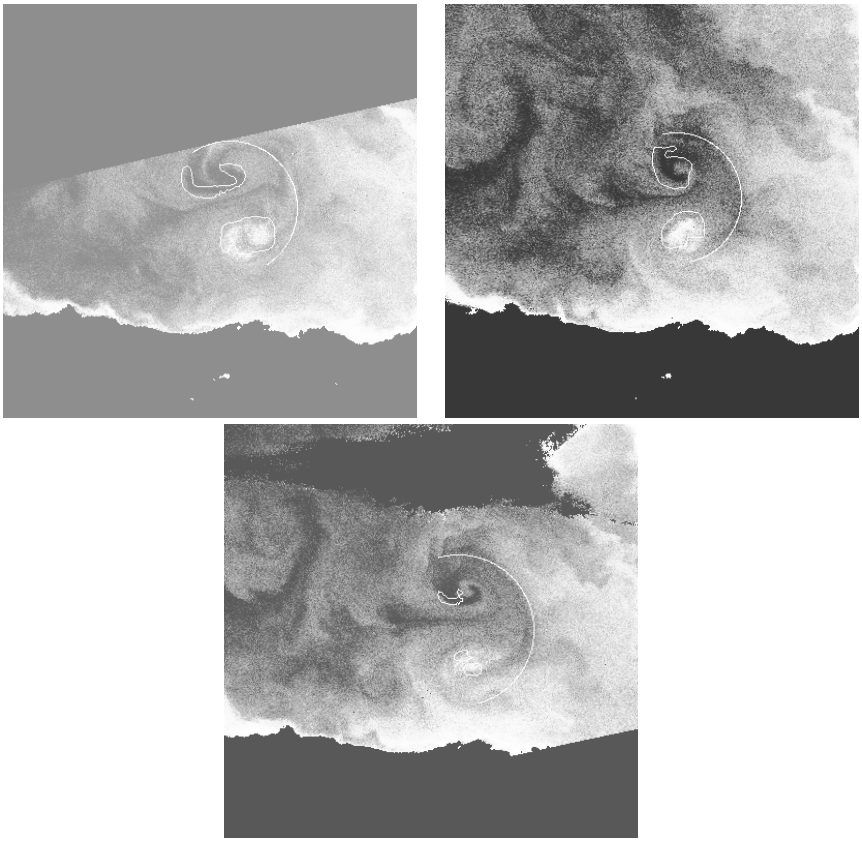

Figure 6: Results obtained on three consecutive CZCS images. An overlay of the obtained model is displayed on each frame.

- consider the problem of data fusion. Information coming from Infra-red data (AVHRR) and color data (CZCS) are highly correlated but contrast and statistical properties of grey level values vary from one sensor to another. Moreover, the stability of the process is different for the different types of data.

7 ACKNOWLEDGEMENTS

We thank ACRI company for providing us AVHRR images under a research contract, and also for giving us information about the data and oceanic structures. The OCEAN (Ocean Color European Archive Network) project is the data source of the CZCS images.

References

[1] Brian G. Schunck. The image flow constraint equation. *Computer Vision, Graphics, and Image Processing*, 35:20–46, 1986.

[2] Berthold K.P. Horn and G. Schunck. Determining optical flow. *Artificial Intelligence*, 17:185–203, 1981.

[3] Solomon Lefschetz. *Differential Equations: Geometric Theory*. Dover Publications, New York, second edition, 1976.

[4] J. Aisbett. Optical flow with an intensity-weighted smoothing. *IEEE Transactions on Pattern Analysis and Machine Intelligence*, 11(5):512–522, May 1989.

[5] Isaac Cohen. Nonlinear variational method for optical flow computation. In *Proceedings of the 8th Scandinavian Conference on Image Analysis*, pages 523–530, Tromso, Norway, June 1993. IAPR.

[6] Chiao-Fe Shu and Ramesh C. Jain. Vector field analysis for oriented patterns. In *IEEE Proceedings of Computer Vision and Pattern Recognition*, pages 673–676, Urbana Champaign, Illinois., June 1992.

[7] A. R. Rao and R. C. Jain. Computerized flow field analysis: Oriented textures fields. *IEEE Transactions on Pattern Analysis and Machine Intelligence*, 14(7):693–709, July 1992.

[8] H. H. Nagel and W. Enkelmann. An investigation of smoothness constraints for the estimation of displacement vector fields from image sequence. *IEEE Transactions on Pattern Analysis and Machine Intelligence*, 8(5):565–593, September 1986.

[9] Ralph M. Ford, Robin N. Strickland, and Bruce A. Thomas. Image models for 2-D flow visualization and compression. *CVGIP: Graphical models and Image Processing*, 56(1):75–93, January 1994.

[10] Jialin Zhong, Thomas S. Huang, and Ronald J. Adrian. Salient structure analysis of fluid flow. In *IEEE Proceedings of Computer Vision and Pattern Recognition*, pages 310–315, Seattle, Washington, June 1994.

[11] Ralph M. Ford and Robin N. Strickland. Nonlinear phase portrait models for oriented textures. In *IEEE Proceedings of Computer Vision and Pattern Recognition*, pages 644–645, New-York, June 1993.